Three-wave mixing of ordinary and backward electromagnetic waves: extraordinary transients in the nonlinear reflectivity and parametric amplification

VITALY V. SLABKO[1], **ALEXANDER K. POPOV**[2,*], **VIKTOR A. TKACHENKO**[1], AND **SERGEY A. MYSLIVETS**[1,3]

[1] *Siberian Federal University, 79 Svobodny Av., Krasnoyarsk, 660041, Russian Federation*
[2] *Birck Nanotechnology Center, Purdue University; 1205 W State Str., West Lafayette, IN 47907, USA*
[3] *L. V. Kirensky Institute of Physics, Siberian Branch of the Russian Academy of Sciences, Krasnoyarsk, 660036, Russian Federation*
*Corresponding author: popov@purdue.edu

Three-wave mixing of ordinary and backward electromagnetic waves in pulsed regime is investigated in the metamaterials which enable the co-existence and phase matching of such waves. It is shown that opposite direction of phase velocity and energy flux in backward waves gives rise to extraordinary transient processes due to greatly enhanced optical parametric amplification and frequency up and down shifting nonlinear reflectivity. The differences are illustrated through comparison with the counterparts in ordinary, co-propagating setting. © 2016 Optical Society of America

Advances in nanotechnology have made possible the engineering of the metamaterials (MMs) which support optical backward electromagnetic waves (BEMWs). Counter-intuitively, energy flux and phase velocity are *contra-directed* in BEMWs. Such waves may exist only in a certain frequency range dependent on particular MM whereas only ordinary EMWs propagate outside the BW frequency band. The emergence of optical BEMWs gives rise to revolutionary breakthroughs in linear photonics and its applications, such as sub-wavelength resolution and cloaking, which are not possible with ordinary optical EMWs [1]. This justifies studies on nonlinear optical (NLO) techniques for excitation and control of BEMWs. Exciting possibilities were predicted in nonlinear photonics, such as huge enhancement in wave mixing through implementation of BEMW as one of the coupled waves [1–3] (and references therein). Extraordinary enhancement in coherent energy transfer from the ordinary pump waves to contra-propagating BEMWs at different frequencies can be employed for compensating losses inherent to BEMWs in plasmonic MMs and to broaden a spectrum of achievable BEMWs and their use in photonics. Among them are ultracompact

optical parametric amplifiers (OPA) and cavity-free optical parametric oscillators (OPO), modulators and all-optically controlled, frequency up and down shifting nonlinear optical reflectors and sensors in optical and microwave ranges of electromagnetic radiation [1–3].

Unparalleled properties of frequency mixing of *ordinary* contra-propagating waves were predicted in the beginning of the NLO era in the early 60s (see, e.g., [4] and references therein). NLO coupling of counterpropagating ordinary optical and acoustic waves was investigated in [5]. Extraordinary properties of photon-phonon coupling of two ordinary optical and one *backward* optical phonon wave were investigated in [6, 7]. Parametric interaction of quasi-phase-matched counterpropagating ordinary optical waves in periodically poled nonlinear crystals was studied theoretically and experimentally in [8–12]. A review of four-wave mixing of ordinary contra-propagating waves in the context of optical phase conjugation is given in [13]. As concerns BEMWs, current mainstream in engineering the MMs which can support BEMWs is to craft the MMs composed of plasmonic mesoatoms which introduce negative μ and ϵ (negative-index MMs, NIMs) [1]. A more broad class of MMs, which can ensure a whole set of the critically important NLO requirements: i) the coexistence and ii) the phase-matching of ordinary and BEMWs which iii) satisfy to the energy conservation law, was recently proposed in [14–18] based on the negative spatial dispersion and nanowaveguide operation regimes. Parametric interaction of ordinary and BEMWs was realized in the microwave transmission lines [19–21]. Miniaturization is intrinsic to MMs. Small NLO coupling volume dictates intense pulse excitation which justifies the investigations described below. This letter is to show fundamental differences in transient regimes in BW and ordinary three-wave mixing (TWM) processes of OPA and difference-frequency generation initiated by the pulse with a sharp forefront.

A remarkable difference in TWM, $\omega_1 = \omega_3 - \omega_2$, in the alternative cases of co- and contra-propagating waves at frequencies ω_1 and ω_2 [Fig.1(a), (b)] is as follows. For co-propagating EMWs coupled in an ordinary loss-free material [Fig.1(a)], a signal at ω_2 grows as $a_2(L) \sim \exp(gL)$. However, this dependence dra-
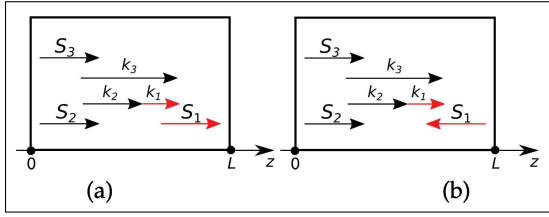
Fig. 1. Two alternative coupling options: (a) – co-propagating waves; (b) – contra-propagating signal and BW idler waves. Here, $\vec{k}_j$ are wave vectors and $\vec{S}_j$ are Poynting vectors.

matically changes to $a_2(L) \sim 1/\cos(gL)$ in the case of Fig. 1(b) [22, 23]. In the latter case, ordinary wave at ω_2 propagates along the pump wave at ω_3 whereas the phase matched idler at ω_1 is a BEMW which propagates in the opposite direction. Here, a_2 is the amplitude of the transmitted signal wave, L is the thickness of the NLO slab, g is a factor proportional to NLO susceptibility and to amplitude a_3 of the pump wave at ω_3. In the latter case, the transmittance T_2 at ω_2, (*OPA*) experiences extraordinary enhancement as $gL \to \pi/2$. This value will be referred to as critical value. The output idler at ω_1 contra-propagating in the *reflection* direction experiences similar huge intensity-resonant enhancement. Such a "geometrical" resonance dependence of the TWM output on L (or on g) occurs due to the *internal distributed NLO feedback* which is intrinsic to the contra-propagating setting. The outlined resonance dependence resembles resonance property of a cavity composed of two mirrors as the cavity length L or wave vector k_q approach resonance values. The latter occurs as two coherent contra-propagating waves meet each other to interfere destructively on the mirrors. Oscillation resonances are known to cause transient processes under pulsed excitation, which is the behavior intrinsic to any oscillator.

This paper is to demonstrate unparalleled transient processes in the BW OPA and in the NLO reflectivity in the vicinity of the resonance intensities of the pump (control) field at ω_3. Such transients are *extraordinary* because they are not inherent to TWM of co-propagating waves in ordinary materials. The outlined *frequency-shifting NLO reflectivity* has no analog in the case of ordinary co-propagating TWM settings too.

Consider interaction of three electromagnetic waves $E_j(z,t) = A_j(z,t)\exp\{i(\omega_j t - k_j z)\}$ (j=1, 2, 3) in a medium slab of length L with quadratic nonlinearity $\chi^{(2)}$. Wave vectors of all waves are co-directed along the axis z. The relations $\omega_3 = \omega_1 + \omega_2$, $k_3 = k_1 + k_2$ and $(A_3 > A_1, A_2)$ are supposed met. After introducing amplitudes $e_j = \sqrt{|\epsilon_j|/k_j}A_j$, $a_j = e_j/e_{30}$, coupling parameters $\text{æ} = \sqrt{k_1 k_2/|\epsilon_1 \epsilon_2|}4\pi\chi_{\text{eff}}^{(2)}$ and $g = \text{æ}A_{30}$, where ε_1 and ε_2 are dielectric permittivity of the medium at the corresponding frequencies, $A_{j0} = A_j(z=0)$, equations for electric components of waves in the approximation of slowly varying amplitudes can be written as:

$$\begin{cases} \partial a_1/\partial z + (1/v_1)\partial a_1/\partial t = -s_1[iga_3 a_2^* + (\alpha_1/2)a_1], \\ \partial a_2/\partial z + (1/v_2)\partial a_2/\partial t = -iga_3 a_1^* - (\alpha_2/2)a_2, \\ \partial a_3/\partial z + (1/v_3)\partial a_3/\partial \tau = -iga_1 a_2 - (\alpha_3/2)a_3. \end{cases} \quad \textbf{(1)}$$

Here, α_j are absorption indices and v_j are group velocities at the corresponding frequencies. For ordinary wave at ω_1 [Fig. 1(a)], $v_1 > 0$, $s_1 = 1$. For BW at ω_1 [Fig. 1(b)], $v_1 < 0$, $s_1 = -1$. Quantities $|a_j|^2$ are proportional to the time dependent photon

fluxes, g^{-1} is a characteristic slab length required for significant NLO energy transfer from the pump field A_3 to the signal at ω_2 and to the idler at ω_1. In the case of Fig. 1(a), the boundary conditions are defined as $a_{10} = 0$, $a_{20} = u$. In the case of Fig. 1(b), they change for $a_{1L} = 0$ and $a_{20} = u$. Here, $u \ll a_{30}$. It is readily seen, e.g. for the ultimate case of continuous wave (CW) regime and $\alpha_j = 0$, that the indicated changes give rise to fundamental transformation of solution to the coupled Eqs. (1) and to appearance of the outlined geometrical resonance instead of exponential dependence [22].

We introduce transmission (OPA) factor $T_2 = |a_{2L}(t)/a_{20}|^2$, and the NLO reflectivity factor $R_1 = |a_{10}(t)/a_{20}|^2$. Basically, two different regimes are possible. In the first one, the input pump A_{30} is a semi-infinite rectangular pulse and the input signal is a CW ($A_{20}=$ const). In the opposite case, the pump is a CW and A_{20} is a semi-infinite rectangular pulse. First, consider the case of $v_3 = v_2 = -v_1 = v$. Shape of semi-infinite pulse with sharp front edge travelling with group velocity v along the axis z is given by function $F(t) = \left\{1 - \tanh\left[(z/v - t)/t_f\right]\right\}/2$, where parameter t_f determines its edge steepness. In the following numerical simulation, it is taken equal to $t_f = 0.05\Delta t$, where $\Delta t = L/v_3$ is a travel time of the fundamental pulse front edge through the slab. In the first case, $a_{30}(t) = a_{30}F(t)$, $a_{20}=$ const. In the second case, $a_{20}(t) = a_{20}F(t)$, $a_{30}=$ const. Here, a_{j0} is a maximum pulse amplitude magnitude at the slab entrance. Solution to Eqs. (1) was obtained through numerical simulations.
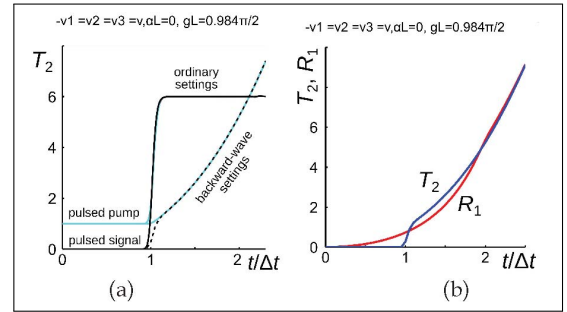

Fig. 2. (a) Difference in the transient processes under ordinary (the solid lines) and BW (the dashed lines) settings. $T_2(t)$ is transmission (OPA) of the co-directed seeding signal at the forefront area of the output signal pulse. (b) Difference in the transient processes in $T_2(t)$ and in nonlinear-optical reflectivity $R_1(t)$ (contra-propagating generated idler) vs time for the case of the pulsed input signal and CW pump. (a) and (b): $-v_1 = v_2 = v_3 = v$, $\alpha_j = 0$, $gL = 0.984\pi/2$.

Figure 2(a), the solid line, depicts output signal at the slab exit ($z = L$) for the case of co-propagating ordinary waves and the dashed line – for the case of BW setting. It is seen that any changes in the output signal occur only after the travel period, both in the ordinary and BW regimes. For the case of pulsed input pump and CW input signal, the output signal experiences amplification when forefront of the pump pulse reaches the exit. For the co-propagating settings, shape of the signal pulse almost follows the shape of the pump pulse. However, in the BW setting, pulse shape changes dramatically in the vicinity of the resonance intensity of the pump wave, which corresponds to $gL = \pi/2$. The signal growth occurs slower, the output signal maximum is greater and is reached with significant delay. Figure 2(b) compares transmitted signal at $z = L$ and the idler

at $z = 0$ traveling in the reflection direction for the case of pulsed input signal and CW pump. It takes travel time Δt for the signal pulse to appear at $z = L$, whereas the idler is generated immediately after the pulse enters the slab. Hence, unlike the transmittance, the transients in the reflectivity are the same for the pulsed signal and pulsed pump modes. Figure 2 (a) and (b) show that differences in OPA for the cases of the pulsed signal and the pulsed pump disappear after a period of time about Δt, whereas the reflectivity and OPA develop in a similar way after a period of time about $2\Delta t$.
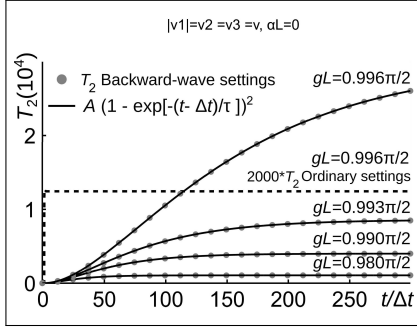
Fig. 3. Dependence of the transient OPA on the intensity of the pump field. The dashed line – TWM of co-propagating waves. Points correspond to ordinary signal and contra-propagating idler. The solid lines depict approximation of the transient OPA by the function $T_2(t) = A\{1 - \exp\left[-(t - \Delta t)/\tau\right]\}^2$. $-v_1 = v_2 = v_3 = v$, $\alpha_j = 0$.

Figure 3 depicts a more extended period of time. It demonstrates that the rise time and the maximum of OPA increase with approaching the resonance strength of the pump field. It also demonstrates the fundamental difference between the rise periods and 8 orders difference in maxima achieved in the ordinary and BW TWM. It appears that calculated data can be approximated by the exponential dependence $T_2(t) = A(1 - \exp\left[-(t - \Delta t)/\tau\right])^2$ (the solid lines), where the rise time τ grows approximately as $1/\cos(gL)$ in the vicinity of the intensity resonance. For example, at $gL = 0.996\pi/2$, the fitting values are $A = 2.99 \cdot 10^4$, $\tau = 109.9\Delta t$. The short initial period (Fig. 2) is not resolved here. As outlined above, the transient processes in OPA and in the NLO reflectivity are similar through the given time period.
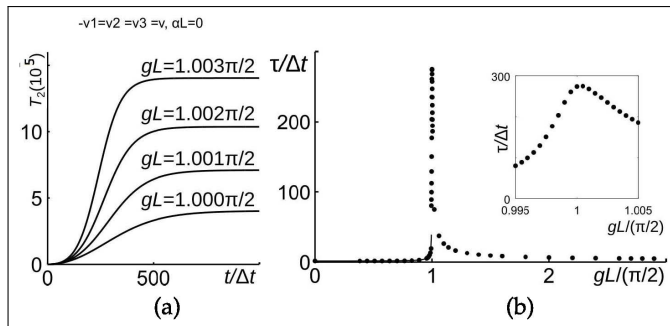
Fig. 4. (a) Shape of the signal forefront in transparent material at pump intensities above the critical input value $gL = \pi/2$. (b) Dependence of the transient period τ on the maximum intensity of the pump field. $-v_1 = v_2 = v_3 = v$, $\alpha_j = 0$.

Distributed NLO feedback gives rise to significant enhance-

ment of the OPA and to depletion of the fundamental wave at $gL > \pi/2$. The latter leads to the stationary regime and to decrease of the transient period (Fig. 4). As seen from Fig. 4(b), the delay of the output signal maximum relative to the pump maximum may reach impressive values on the order of hundreds of the travel periods Δt. Maximum delay is reached at $gL = \pi/2$.
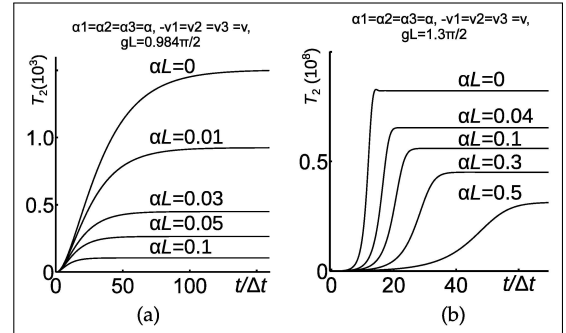
Fig. 5. Effect of absorption on the transient OPA for two different intensities of the pump field. $-v_1 = v_2 = v_3 = v$. $\alpha_1 = \alpha_2 = \alpha_3 = \alpha$. (a) $gL = 0.984\pi/2$. (b) $gL = 1.3\pi/2$.

Absorption causes change in the delay time. For the case of CW and neglected depletion of the pump, parameter g must be replaced by $g_{eff} = \sqrt{g^2 - (\alpha_1 + \alpha_2)^2/16}$ [23]. Hence, losses shift maximum delay to $gL > \pi/2$ as seen in Figs. 5 and 6(a).
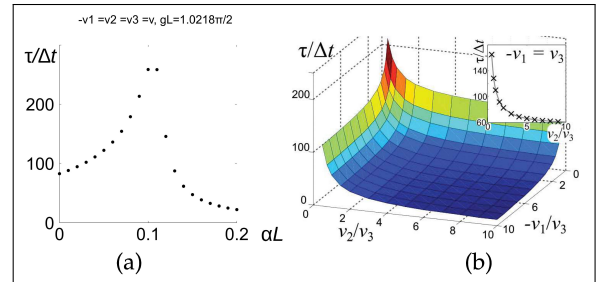
Fig. 6. a) Effect of absorption on the transient period. $gL = 1.0218\pi/2$, $-v_1 = v_2 = v_3 = v$, $\alpha_1 = \alpha_2 = \alpha$, $\alpha_3 = 0$. (b) Dependence of duration of the transient period in TWM on the group velocities of the coupled waves and on their dispersion. $\alpha_j = 0$, $gL = 0.996\pi/2$.
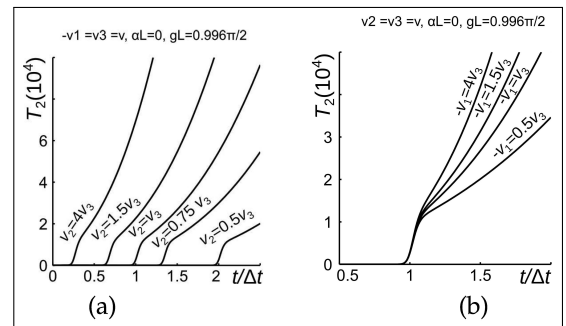
Fig. 7. Dependence of the transient TWM on the forefront of the output pulses on dispersion of group velocities of the coupled waves. $gL = 0.996\pi/2$, $\alpha_j = 0$. (a) $-v_1 = v_3$. (b) $v_2 = v_3$.

Transient period increases with the decrease of the group velocities (in the slow light regimes) as shown in Fig. 6(b). Figures 7 (a) and (b) depict dependence of the transient processes at the forefront of the output signal on the dispersion of group velocities. Figure 7(a) shows that the forefront of the output signal becomes steeper if it outruns the pump pulse. Figure 7(b) demonstrates that the pulse forefront also becomes steeper with an increase of the group velocity for the idler.

In the **conclusion**, we report extraordinary transient processes in optical parametric amplification and in the frequency-shifting nonlinear optical reflectivity. They originate from the three-wave mixing where one of the coupled waves travels against others. An example is investigated where the signal and the pump are ordinary co-propagating waves and the idler is the contra-propagating backward wave. Phase-matching is supposed achieved, i.e. all waves travel with the same phase velocities. The reference is given to the works showing how such a requirement can be satisfied. Energy flux (the group velocity) and the phase velocity are counter-directed in the backward wave. In this case, the phase matching dictates energy flux in the backward wave (here, in the idler) to be directed against those in the pump and signal, i.e., in the reflection direction. Such coupling geometry gives rise to greatly enhanced coherent energy transfer from the pump to the signal and to the contra-propagating idler. We show that the enhanced coupling causes the transient processes in the three-wave mixing that have no analogs in the case of co-propagating couplings. Two options are investigated where the input pump is pulsed, whereas the input signal is a continuous wave and vice versa. For the sake of explicitness, the ultimate case is investigated of a semi-infinite pulse with sharp rectangular forefront entering a metamaterial slab. In both cases, the contra-propagating signal and idler, which exit the metaslab from the opposite sides, also appear semi-infinite pulses, however, with the forefront significantly different from that of the input pulse. The results are contrasted by comparing with the similar processes in the ordinary materials under standard settings where all coupled waves are co-propagating. The effects of changing the pump intensity, material absorption and the group velocities dispersion on the transient processes are investigated.

The major conclusions are as follows. There exist resonance value of the input pump intensity which depends on the nonlinear susceptibility and on the thickness of the metaslab. Indicated extraordinary resonance provides giant enhancement in the three-wave coupling. Consequently, great enhancement occurs in optical parametric amplification of the signal and in the oppositely directed idler (in the frequency up or down shifted reflectivity). Such effect does not exist in the ordinary optical parametric amplification in the case of all co-directed energy fluxes, where the indicated reflectivity does not exist at all. In the vicinity of the resonance intensity, extraordinary transient processes develop which cause a change in the output pulse shapes and a significant delay of their maximums. The latter is not the case under co-propagating setting. The closer pump intensity approaches the resonance value, the longer becomes the transient period. The delay in the output pulses maximums relative to the input ones may occur up to several hundred times longer than the travel time of the fundamental pulse through the metaslab. A difference between the case of the input pulsed pump and the case of the input pulsed signal disappears after the time period of about travel time for the fundamental pulse. Reflected pulse begins to develop immediately after the pump or the seeding pulse edges enter the slab, whereas the pulse in the amplified signal begins to form with the delay of about the travel time. Depletion of the pump at the input intensities above the resonance value causes a decrease in the rise time, which therefore has a maximum as a function of the input pulse intensity. Losses cause shift of the maximum delay time to higher input pump intensities. Dispersion in the modules of the group velocities causes changes in the transient processes as well, which significantly depends on the particular difference between the group velocities of the coupled pulses.

The outlined coupling scheme and the revealed unparalleled properties must be accounted for at creation of advanced all-optically controlled optical amplifiers, filters, modulators, reflectors and sensors implementing backward electromagnetic waves. Similar processes are anticipated for the three-wave mixing of the ordinary contra-propagating waves achievable in crystals through quasi-phase matching [8–12] and for the optical phase conjugation [13].

REFERENCES

1. W. Cai and V. Shalaev, *Optical metamaterials, fundamentals and applications*, Springer-Verlag New York, 2010.
2. A. K. Popov and V. M. Shalaev, in *Metamaterials: Fundamentals and Applications IV*, Alan D. Boardman, Nader Engheta, Mikhail A. Noginov, Nikolay I. Zheludev, Editors: Proc. SPIE, **8093**, 809306-27 (2011).
3. A. K. Popov, Nonlinear Optics with Backward Waves, ch. 10, pp. 193-213, in *Nonlinear, Tunable and Active Metamaterials*, Ilya V. Shadrivov, Mikhail Lapine and Yuri S. Kivshar Editors, Springer (2015).
4. S. E. Harris, Appl. Phys. Lett. **9**, 114 - 116 (1966).
5. D. L. Bobroff, J. Appl. Phys. **36**, 1760 (1965).
6. M. I. Shalaev, V. V. Slabko, S. A. Myslivets, A. K. Popov, Opt. Lett. **36**, 3861 − 3863 (2011).
7. A. K. Popov, M. I. Shalaev, S. A. Myslivets, V. V. Slabko, and I. S. Nefedov, Appl. Phys. A **115**, 523 - 529 (2014).
8. Y. J. Ding and J. B. Khurgin, IEEE J. Quantum Electron. **32**, 1574 − 1582 (1996).
9. Y. J. Ding and J. B. Khurgin, Opt. Lett. **21**, 1445 - 1447 (1996).
10. C. Conti and G. Assanto, Opt. Lett. **24**, 1139 - 1141 (1999).
11. C. Canalias, V. Pasiskevicius, Nat. Photonics, **1**, 459 - 462 (2007).
12. J. B. Khurgin, Nat. Photonics, **1**, 446 - 447 (2007).
13. B. Ya. Zel'dovich, N. F. Pilipetsky, V. V. Shkunov, *Principles of Phase Conjugation* (Springer Series in Optical Sciences, **42**, 1985), Ch. 6.
14. A. K. Popov, M. I. Shalaev, S. A. Myslivets, V. V. Slabko, and I. S. Nefedov, Appl. Phys. A **109**, 835 - 840 (2012).
15. A. K. Popov, I. S. Nefedov, S. A. Myslivets, M. I. Shalaev, V. V. Slabko, Proc. SPIE **8725**, 87252E (2013).
16. A. K. Popov, V. V. Slabko, M. I. Shalaev, I. S. Nefedov, and S. A. Myslivets, Solid State Phenomena **213**, 222–225 (2014).
17. A. K. Popov, I. S. Nefedov, and S. A. Myslivets, arXiv:1602.02497.
18. C. Duncan, L. Perret, S. Palomba, M. Lapine, B. T. Kuhlmey, and C. M. de Sterke, Scientific Reports **5**, 08983 (2015).
19. K. I. Volyak and A. S. Gorshkov, Radioteknika i Elektronika **18** (10), 2075 - 2082 (1973) (in Russian).
20. A. B. Kozyrev, H.Kim, and D. W. van der Weide, Appl. Phys. Lett. **88**, 264101 (2006).
21. A. Rose, D. Huang, and D. R. Smith, Phys. Rev. Lett. **107**, 063902 (2011).
22. A. Yariv, *Quantum Electronics*, 3rd ed. (Wiley, New York, 1988), p. 466.
23. A. K. Popov and V. M. Shalaev, Appl. Phys. B Lasers Opt. **84**, 131 − 137 (2006).

amplification," Appl. Phys. B Lasers Opt. **84**, 131 – 137 (2006).

REFERENCES

1. W. Cai and V. Shalaev, "Optical metamaterials, fundamentals and applications", Springer-Verlag New York, 2010.
2. A. K. Popov and V. M. Shalaev, "Merging nonlinear optics and negative-index metamaterials," in *Metamaterials: Fundamentals and Applications IV*, Alan D. Boardman, Nader Engheta, Mikhail A. Noginov, Nikolay I. Zheludev, Editors: Proc. SPIE, **8093**, 809306-27 (2011).
3. A. K. Popov, "Nonlinear Optics with Backward Waves", ch. 10, pp. 193-213, in Nonlinear, Tunable and Active Metamaterials, Ilya V. Shadrivov, Mikhail Lapine and Yuri S. Kivshar Editors, Springer (2015), DOI 10.1007/978-3-319-08386-5.
4. S. E. Harris "Proposed backward wave oscillation in the infrared," Appl. Phys. Lett. **9**, 114 - 116 (1966), http://dx.doi.org/10.1063/1.1652520.
5. D. L. Bobroff "Coupled Modes Analysis of the Phonon Photon Parametric Backward Wave Oscillator," J. Appl. Phys. **36**, 1760 (1965), http://dx.doi.org/10.1063/1.1703124.
6. M. I. Shalaev, V. V. Slabko, S. A. Myslivets, A. K. Popov,"Negative group velocity and three-wave mixing in dielectric crystals," Opt. Lett. **36**, 3861 – 3863 (2011).
7. A. K. Popov, M. I. Shalaev, S. A. Myslivets, and V. V. Slabko, "Unidirectional amplification and shaping of optical pulses by three-wave mixing with negative phonons," Appl. Phys. A **115**, 523 - 529 (2014).
8. Y. J. Ding and J. B. Khurgin, "Backward optical parametric oscillators and amplifiers," IEEE J. Quantum Electron. **32**, 1574 – 1582 (1996).
9. Y. J. Ding and J. B. Khurgin "Second-harmonic generation based on quasi-phase matching: a novel configuration," Opt. Lett. **21**, 1445 - 1447 (1996).
10. C. Conti and G. Assanto, "Cavityless oscillation through backward quasi-phase-matched second-harmonic generation," Opt. Lett. **24**, 1139 - 1141 (1999).
11. C. Canalias, V. Pasiskevicius, "Mirrorless optical parametric oscillator," Nat. Photonics, **1**, 459 - 462 (2007) doi:10.1038/nphoton.2007.137.
12. J. B. Khurgin, "Optical parametric oscillator: Mirrorless magic," Nat. Photonics, **1**, 446 - 447 (2007) doi:10.1038/nphoton.2007.131.
13. B. Ya. Zel'dovich, N. F. Pilipetsky, V. V. Shkunov, *Principles of Phase Conjugation* (Springer Series in Optical Sciences, vol. 42, 1985, doi: 10.1007/978-3-540-38959-0), chapter 6.
14. A. K. Popov, M. I. Shalaev, S. A. Myslivets, V. V. Slabko, and I. S. Nefedov, "Enhancing coherent nonlinear-optical processes in nonmagnetic backward-wave materials," Appl. Phys. A **109**, 835 - 840 (2012), doi:10.1007/s00339-012-7390-8.
15. A. K. Popov, I. S. Nefedov, S. A. Myslivets, M. I. Shalaev, V. V. Slabko, "Nonlinear-optical up and down frequency-converting backward-wave metasensors and metamirrors," Proc. SPIE 8725, *Micro- and Nanotechnology Sensors, Systems, and Applications V*, 87252E (2013); doi:10.1117/12.2015637.
16. A. K. Popov, V. V. Slabko, M. I. Shalaev, I. S. Nefedov, and S. A. Myslivets, "Nonlinear optics with backward waves: Extraordinary features, materials and applications," Solid State Phenomena **213**, 222–225 (2014), doi:10.4028/www.scientific.net/SSP.213.222.
17. A. K. Popov, I. S. Nefedov, and S. A. Myslivets, "Phase matched backward-wave second harmonic generation in a hyperbolic carbon nanoforest," arXiv:1602.02497.
18. C. Duncan, L. Perrel, S. Palomba, M. Lapine, B. T. Kuhlmey, and C. M. de Sterke, "New avenues for phase matching in nonlinear hyperbolic metamaterials," Scientific Reports **5**, 08983 (2015).
19. K. I. Volyak and A. S. Gorshkov, "Investigation of backward-wave parametric generator," Radioteknika i Elektronika **18** (10), 2075 - 2082 (1973) (in Russian), UDK 621.373.7.001.5
20. A. B. Kozyrev, H.Kim, and D. W. van der Weide, "Parametric amplification in left-handed transmission line media," Appl. Phys. Lett. **88**, 264101 (2006), DOI: 10.1063/1.2214136.
21. A. Rose, D. Huang, and D. R. Smith, "Controlling the second harmonic in a phase-matched negative-index metamaterial," Phys. Rev. Lett. **107**, 063902 (2011).
22. A. Yariv, Quantum Electronics, 3rd ed. (Wiley, New York, 1988), p. 466.
23. A. K. Popov and V. M. Shalaev, "Negative-index metamaterials: second harmonic generation, Manley - Rowe relations and parametric